NASA TECHNICAL NOTE

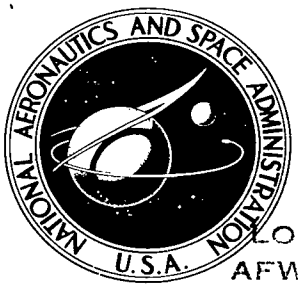

NASA TN D-8325

FRACTURE ANALYSIS OF SURFACE AND THROUGH CRACKS IN CYLINDRICAL PRESSURE VESSELS

J. C. Newman, Jr.

Langley Research Center
Hampton, Va. 23665

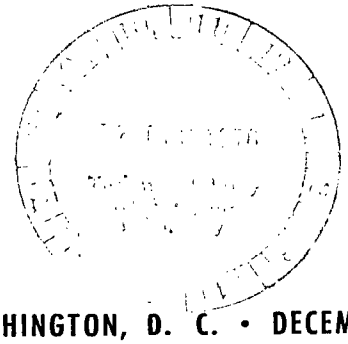

NATIONAL AERONAUTICS AND SPACE ADMINISTRATION • WASHINGTON, D. C. • DECEMBER 1976

1. Report No. NASA TN D-8325	2. Government Accession No.	3. Recipient's Catalog No.
4. Title and Subtitle FRACTURE ANALYSIS OF SURFACE AND THROUGH CRACKS IN CYLINDRICAL PRESSURE VESSELS		5. Report Date December 1976 6. Performing Organization Code
7. Author(s) J. C. Newman, Jr.		8. Performing Organization Report No. L-11118
9. Performing Organization Name and Address NASA Langley Research Center Hampton, VA 23665		10. Work Unit No. 505-02-31-01 11. Contract or Grant No.
12. Sponsoring Agency Name and Address National Aeronautics and Space Administration Washington, DC 20546		13. Type of Report and Period Covered Technical Note 14. Sponsoring Agency Code
15. Supplementary Notes		

16. Abstract

A previously developed fracture criterion was applied to fracture data for surface- and through-cracked cylindrical pressure vessels to see how well the criterion can correlate fracture data. Fracture data from the literature on surface cracks in aluminum alloy, steel, and epoxy vessels, and on through cracks in aluminum alloy, titanium alloy, steel, and brass vessels were analyzed by using the fracture criterion. The criterion correlated the failure stresses to within ±10 percent for either surface or through cracks over a wide range of crack size and vessel diameter. The fracture criterion was also found to correlate failure stresses to within ±10 percent for flat plates (center-crack or double-edge-crack tension specimens) and cylindrical pressure vessels containing through cracks.

17. Key Words (Suggested by Author(s))
Fracture
Stress-intensity factor
Structural mechanics
Materials (metallic)

18. Distribution Statement
Unclassified - Unlimited

Subject Category 39

19. Security Classif. (of this report)	20. Security Classif. (of this page)	21. No. of Pages	22. Price*
Unclassified	Unclassified	33	$3.75

* For sale by the National Technical Information Service, Springfield, Virginia 22161

FRACTURE ANALYSIS OF SURFACE AND THROUGH CRACKS IN CYLINDRICAL PRESSURE VESSELS

J. C. Newman, Jr.
Langley Research Center

SUMMARY

A previously developed fracture criterion was applied to fracture data for surface- and through-cracked cylindrical pressure vessels to see how well the criterion can correlate fracture data. Fracture data from the literature on surface cracks in aluminum alloy, steel, and epoxy vessels, and on through cracks in aluminum alloy, titanium alloy, steel, and brass vessels were analyzed by using the fracture criterion. The criterion correlated the failure stresses to within ±10 percent for either surface or through cracks over a wide range of crack size and vessel diameter. The fracture criterion was also found to correlate failure stresses to within ±10 percent for flat plates (center-crack or double-edge-crack tension specimens) and cylindrical pressure vessels containing through cracks.

INTRODUCTION

Failures of many pressure vessels have been traced to surface cracks or to through cracks. These cracks initiate at structural discontinuities such as holes, material defects, or other abrupt changes in configuration and may propagate to failure under operating stress levels. To prevent such failures, the designer must be able to predict the effects of crack size on structural strength. Linear elastic fracture mechanics (LEFM), which utilizes the concept of the elastic stress-intensity factor, has been used to correlate fracture data and predict failure for cracked plates and structural components when the crack-tip plastic deformations are constrained to small regions (plane-strain fracture, ref. 1). However, when plastic deformations near the crack tip are large (plastic zone greater than plate thickness) the elastic stress-intensity factor at failure K_{Ie} varies with crack size and structural dimensions. (See refs. 2 to 4.) To account for the variation in K_{Ie} with structural dimensions, the elastic-plastic stress-strain behavior at the crack tip must be considered.

An equation which accounts for the effects of plastic deformation on fracture was derived and is presented in references 4 and 5. This equation relates K_{Ie} to the elastic nominal failure stress and two material fracture parameters and is designated the two-parameter fracture criterion (TPFC). The TPFC has correlated fracture data for surface and through cracks, for different specimen types, and for a wide range of materials (refs. 4 to 7).

The purpose of this paper is to apply the TPFC to surface- and through-cracked cylindrical shells subjected to internal pressure (fig. 1) to see how well the TPFC can correlate such fracture data. Fracture data for pressurized cylinders made of various materials (aluminum alloy, titanium alloy, steel, brass, and epoxy) were taken from the literature. (See table I and refs. 8 to 17.) Some of the literature sources reported fracture data on flat plates (fig. 2) in addition to the data for cylinders. To determine whether or not the failure stresses in the cylinders may be predicted using fracture data for the flat plates, experimental and predicted failure stresses in the flat plates were compared. The predicted failure stresses were computed using the two material fracture parameters determined from the cylinder data. In order to apply the TPFC to fracture data, the elastic stress-intensity factors for these crack configurations must be known.

The elastic stress-intensity factors for through cracks in pressurized cylinders have been obtained theoretically by Folias (ref. 18), and Erdogan and Kibler (ref. 19) for crack lengths less than about five times the square root of the product of vessel radius and thickness. In this paper an empirical equation giving elastic stress-intensity factors for through cracks has been obtained using the numerical results from reference 19 and some experimental fracture tests on brass vessels from reference 16. The resulting equation applies over a range of crack lengths about twice as large as those considered in references 18 and 19.

The elastic stress-intensity factors for surface cracks in pressurized cylinders have not been obtained theoretically, but some experimental stress-intensity factors have been determined from surface cracks in brittle epoxy vessels (ref. 17). In this paper an empirical equation giving elastic stress-intensity factors for surface cracks has been developed using the results from references 4 and 19. The results from this equation are compared with the experimental stress-intensity factors from reference 17.

SYMBOLS

a	initial depth of surface crack, m
c	initial length of surface or through crack (see figs. 1 and 2), m
F	complete boundary-correction factor on the stress intensity
f_t	shell-curvature correction factor for a through crack
f_s	shell-curvature correction factor for a surface crack
H	height of uniformly stressed specimens, m
K_F	fracture toughness, $N/m^{3/2}$
K_I	elastic stress-intensity factor, $N/m^{3/2}$
K_{Ie}	elastic stress-intensity factor at failure, $N/m^{3/2}$

M_e combined front-face and back-face correction on the stress-intensity factor for the surface crack

M_1 front-face correction on the stress-intensity factor for the surface crack

m fracture-toughness parameter

p internal pressure, Pa

Q elastic surface-crack shape factor

R internal radius of cylindrical pressure vessel, m

S_g gross section stress at failure, Pa

S_n nominal (net section) stress at failure, Pa

S_u nominal stress required to produce a plastic hinge on net section ($S_u = \sigma_u$ for center-crack and double-edge-crack tension specimens and $S_u = 1.15\sigma_u$ for pressurized cylinders), Pa

T temperature, K

t shell thickness, m

W specimen width, m

λ_t through-crack shell parameter, $\frac{c}{\sqrt{Rt}}$

λ_s surface-crack shell parameter, $\frac{c}{\sqrt{Rt}}\left(\frac{a}{t}\right)$

ν Poisson's ratio

σ_u ultimate tensile strength (uniaxial), Pa

σ_y yield stress (uniaxial), Pa

ϕ ratio of K_{Ie} to K_F

TWO-PARAMETER FRACTURE CRITERION

The two-parameter fracture criterion (TPFC) was developed and successfully applied to plane fracture specimens containing either surface or through cracks in metallic materials (refs. 4 to 7). The TPFC accounts for the effects of plastic deformation on fracture properties. The equation is

$$K_F = \frac{K_{Ie}}{1 - m\left(\frac{S_n}{S_u}\right)} \qquad (S_n \leq \sigma_y) \qquad (1)$$

where K_{Ie} is the elastic stress-intensity factor at failure, S_n is the nominal (net-section) failure stress, S_u is the nominal stress required to produce a plastic hinge on the net section using the ultimate tensile strength, and K_F and m are the two material fracture parameters. The fracture parameters K_F and m are assumed to be constant for a given combination of material, thickness, temperature, and rate of loading. Three conditions are necessary to obtain fracture parameters that are representative for a given material and test temperature: (1) the nominal failure stress must be less than σ_y, (2) the fracture data must all be from the same specimen thickness, and (3) the test data must encompass a wide range of crack lengths or specimen sizes. Reference 4 shows how the fracture parameters are determined by a least-squares procedure for a given set of fracture data. To define the complete fracture behavior for a material, K_F and m must be determined as functions of thickness, temperature, and load rate.

If m equals zero in equation (1), K_F equals the elastic stress-intensity factor at failure and the equation applies to low-toughness (low K_F) materials (plane-strain fracture). However, if m equals unity, the equation applies to extremely ductile or high-toughness (high K_F) materials. Thus, the fracture parameters, K_F and m, jointly describe the crack sensitivity of the material.

The denominator in equation (1) reflects the influence of the nominal failure stress on fracture toughness. The variation of the denominator with nominal stress for a typical material is shown in figure 3. When the nominal stress is less than the uniaxial yield stress σ_y, the function ϕ (ratio of K_{Ie} to K_F) is a linear function of nominal stress. However, when the nominal failure stress is greater than the yield stress, the function ϕ becomes nonlinear and is dependent upon the stress-strain curve of the material and the state of stress in the crack-tip region (refs. 4 and 6). For thin materials, where the state of stress in the crack-tip region is biaxial, the expected behavior is estimated by the dash-dot curve. An equation approximating the dash-dot curve is given in reference 6 by

$$\phi = \frac{K_{Ie}}{K_F} = \frac{\sigma_y}{S_n}\left(1 - m\,\frac{S_n}{S_u}\right) \qquad (\sigma_y < S_n < S_u) \qquad (2)$$

and is shown in figure 3 as the dashed curve. For thick materials, where the state of stress in the crack-tip region is triaxial, the fracture behavior for $S_n > \sigma_y$ is expected to lie closer to the solid line. The solid vertical line truncates the nominal stress at S_u. In this paper, equation (2) was used whenever S_n was greater than σ_y.

In order to apply equation (1) to surface and through cracks in pressurized cylinders, the nominal stress required to fail the uncracked vessel S_u and the elastic stress-intensity factor K_{Ie} for these configurations must be determined. For pressurized cylinders, S_u was 1.15 times the ultimate tensile strength σ_u. It was determined by calculating the nominal (hoop) stress required to satisfy the Mises yield criterion (where σ_y was replaced by σ_u) assuming a 2:1 biaxial stress ratio. The elastic stress-intensity factor equations for these configurations are presented in the next section.

ELASTIC STRESS-INTENSITY FACTORS

The form of the elastic stress distribution near a crack tip that contains the stress-intensity factor K_I and the square-root singularity is well known (ref. 2). (The determination of K_I is the basis for linear elastic fracture mechanics.) The stress-intensity factor is a function of load, structural configuration, and the size, shape, and location of the crack. In general, the elastic stress-intensity factor can be expressed as

$$K_{Ie} = S_n\sqrt{\pi c}\, F \tag{3}$$

for any Mode I crack configuration where S_n is the nominal stress, c is the initial crack length (defined in figs. 1 and 2), and F is the boundary-correction factor. The boundary-correction factor accounts for the influence of various boundaries and crack shape on stress intensity. The following sections give the nominal stress equation and the boundary-correction factor equations for the surface- and through-cracked cylindrical pressure vessel.

Through Crack in a Thin Pressurized Cylinder

For the through crack (axial) in a cylindrical shell subjected to internal pressure (fig. 1(a)), the elastic stress-intensity factor at failure is given by equation (3) where the nominal stress is

$$S_n = \frac{pR}{t} \tag{4}$$

and

$$F = f_t = \left(1 + 0.52\lambda_t + 1.29\lambda_t^2 - 0.074\lambda_t^3\right)^{1/2} \tag{5}$$

for $0 \leqq \lambda_t \leqq 10$ where $\lambda_t = c/\sqrt{Rt}$. Equation (5) accounts for the effects of shell curvature (refs. 18 and 19) on stress intensity. Poisson's ratio was assumed to be 1/3. The details on the development of equation (5) are given in the appendix.

Surface Crack in a Thin Pressurized Cylinder

For the internal or external surface crack (axial) in a cylindrical shell subjected to internal pressure (fig. 1(b)), the elastic stress-

intensity factor at failure is also given by equation (3), where the nominal stress is given by equation (4) and

$$F = \sqrt{\frac{a}{cQ}}\, M_e f_s \tag{6}$$

The square-root term converts the through-crack expression to that for a surface crack, M_e is the combined front-face and back-face correction factor, and f_s is the shell-curvature correction factor for a surface crack. The elastic shape factor Q was given in reference 20 as the square of the elliptic integral of the second kind. An expression was chosen in reference 4 as a simple approximation for Q and is given by

$$\left.\begin{aligned} Q &= 1 + 1.47\left(\frac{a}{c}\right)^{1.64} && \left(\frac{a}{c} \leqq 1.0\right) \\ Q &= 1 + 1.47\left(\frac{c}{a}\right)^{1.64} && \left(\frac{a}{c} > 1.0\right) \end{aligned}\right\} \tag{7}$$

The expression for M_e (ref. 4) is given by

$$M_e = \left[M_1 + \left(\sqrt{Q\,\frac{c}{a}} - M_1\right)\left(\frac{a}{t}\right)^q\right] \tag{8}$$

where q was determined empirically as

$$q = 2 + 8\left(\frac{a}{c}\right)^3 \tag{9}$$

The term M_1 is the front-face correction, and the a/t term is the back-face correction. The expression for M_1 is given by

$$\left.\begin{aligned} M_1 &= 1.13 - 0.1\left(\frac{a}{c}\right) && \left(0.02 \leqq \frac{a}{c} \leqq 1.0\right) \\ M_1 &= \sqrt{\frac{c}{a}}\left(1 + 0.03\,\frac{c}{a}\right) && \left(\frac{a}{c} > 1.0\right) \end{aligned}\right\} \tag{10}$$

The shell-curvature correction factor for a surface crack f_s is given by

$$f_s = \left(1 + 0.52\lambda_s + 1.29\lambda_s^2 - 0.074\lambda_s^3\right)^{1/2} \tag{11}$$

for $0 \leqq \lambda_s \leqq 10$ where $\lambda_s = \frac{c}{\sqrt{Rt}} \frac{a}{t}$. Again, Poisson's ratio was assumed to be 1/3. The form of λ_s was obtained by assuming that the surface crack could be replaced by an "equivalent" through crack of equal area. As a/t approaches unity, λ_s approaches λ_t and equation (6) reduces to equation (5). In the appendix, equation (6) is compared with some experimentally-determined correction factors for a brittle epoxy.

Through Crack in Axially Loaded Flat Plates

Center-crack tension.- For the center-crack tension specimen (fig. 2(a)), the elastic stress-intensity factor is given by equation (3) where

$$S_n = \frac{S_g}{1 - \frac{2c}{W}} \tag{12}$$

and

$$F = \left(1 - \frac{2c}{W}\right)\sqrt{\sec \frac{\pi c}{W}} \tag{13}$$

for $0 \leqq 2c/W < 1.0$ and $H/W \geqq 2$. The secant term is the finite-width correction on stress-intensity factor and was obtained from reference 1.

Double-edge-crack tension.- For the double-edge-crack tension specimen (fig. 2(b)), the elastic stress-intensity factor is given by equation (3), where S_n is given by equation (12), and F was obtained by a boundary-collocation analysis of a configuration with $H/W = 0.625$. (Fracture data analyzed from ref. 15 used this particular configuration.) The stress S_g was assumed to be uniformly applied. An equation fit to the collocation results gave

$$F = 1.13\left(1 - \frac{2c}{W}\right)\sqrt{\sec \frac{\pi c}{W}} \tag{14}$$

for $0 \leqq 2c/W \leqq 0.4$ and $H/W = 0.625$. (Stress-intensity factors for $H/W = 1$, 3, and ∞ are given in ref. 2.)

ANALYSIS OF FRACTURE DATA

Fracture data on pressurized cylinders made of various materials and containing either surface or through cracks were taken from the literature and were analyzed using the TPFC (eqs. (1) and (2)). The fracture parameters, K_F and m, for a given material, thickness, and test temperature were determined from the fracture data using a best-fit procedure described in reference 4. These values of K_F and m were then used to calculate failure stresses for the same fracture tests to see how well the TPFC correlated the failure stresses. Where fracture data on flat plates (center-crack tension or edge-crack tension) were available, experimental and predicted failure stresses for the flat plates were compared. The failure stresses were computed using the two material fracture parameters determined from the cylinder data. The failure stresses were calculated by substituting equation (3) into equations (1) and (2), and were given by

$$S_n = \frac{K_F}{\sqrt{\pi c}\, F + \frac{mK_F}{S_u}} \qquad (S_n \leqq \sigma_y) \tag{15}$$

and

$$S_n = \sqrt{(m\gamma)^2 + 2\gamma S_u} - m\gamma \qquad (\sigma_y < S_n < S_u) \tag{16}$$

where

$$\gamma = \frac{K_F \sigma_y}{2S_u\sqrt{\pi c}\, F} \tag{17}$$

Table I summarizes the materials, thicknesses, test temperatures, and crack configurations that were analyzed. Figures 4 to 15 show the correlation obtained for each set of fracture data. Table I also indicates which fracture data were obtained using sharp saw-cut slits instead of fatigue cracks.

Through Cracks

Pressurized cylinders.- Figures 4 to 7 show fracture data on pressurized cylinders containing through cracks. The figures show the nominal failure stress normalized to S_u ($1.15\sigma_u$) plotted against half-length of crack c. The symbols show the fracture data, and the curves indicate the best fit of the TPFC using the values of K_F and m determined from these data. A knee occurs in all curves when the nominal stress is equal to the yield stress of the material (transition from eq. (15) to eq. (16)), but some are hardly perceptible. The calculated failure stresses were generally within ±10 percent of the experimental failure stresses.

Pressurized cylinders and flat plates.- Figures 8 to 13 show fracture data on pressurized cylinders and flat plates. In each figure the results are for cylinders and flat plates made of the same material and thickness, and tested at the same temperature. Both the cylinders and flat plates contained through cracks. The figures show nominal failure stress normalized to S_u plotted against half-length of crack c. For the flat plates $S_u = \sigma_u$ and for the cylinders $S_u = 1.15\sigma_u$. The fracture parameters, K_F and m, were determined from an analysis of the fracture data on the pressurized cylinders. The fracture data on the flat plates were insufficient to obtain the two parameters because only one specimen size and crack length was tested. The solid curve or curves show the calculations from the TPFC for various vessel radii. The agreement was considered good. The dashed curve on each figure shows the predicted results for flat plates ($R = \infty$) using the values of K_F and m determined from the cylinders. The circular symbols show the experimental results for the flat plates. The predicted results were within ±10 percent of the experimental failure stresses.

Surface Cracks

Pierce (ref. 11) conducted cryogenic fracture tests on surface cracks in 2014-T6 material. Figure 14 shows S_n normalized to S_u ($1.15\sigma_u$) plotted against cF^2, where c is the half-length of crack and F is the boundary-correction factor (eq. (6)). The TPFC indicates that this type of plot (S_n/S_u against cF^2) gives a single curve for various a/c and a/t ratios. The open and solid circular symbols denote experimental data on externally or internally located surface cracks, respectively. The surface-crack data included variations in crack shape $\left(0.07 \leqq \frac{a}{c} \leqq 0.9\right)$ and crack size $\left(0.36 \leqq \frac{a}{t} \leqq 0.98\right)$. The curve shows the calculations from the TPFC using the values of K_F and m determined from these data. The calculated failure stresses were within ±10 percent of the experimental failure stresses.

Kiefner, Maxey, Eiber, and Duffy (ref. 14) conducted surface-crack fracture tests at room temperature on steel pressure vessels. Figure 15 shows the nominal failure stresses normalized to S_u plotted against cF^2. The surface-crack data included variations in crack shape $\left(0.02 \leqq \frac{a}{c} \leqq 0.14\right)$ and crack size $\left(0.38 \leqq \frac{a}{t} \leqq 0.82\right)$. The symbols denote the fracture data and the the curve shows the calculations from the TPFC. The agreement was considered good.

CONCLUDING REMARKS

A two-parameter fracture criterion that relates the elastic stress-intensity at failure, the elastic nominal failure stress, and two material

parameters was used to analyze fracture data on surface- and through-cracked cylindrical pressure vessels. Fracture data from the literature on steel, titanium alloy, aluminum alloy, brass, and epoxy vessels tested at either room or cryogenic temperature were analyzed. The two-parameter fracture criterion correlated the data well (generally within ±10 percent of the experimental failure stresses) for a broad range of materials, including some that were extremely ductile. The fracture criterion was also found to correlate fracture data from flat plates and cylindrical pressure vessels within ±10 percent for the same material, thickness, and test temperature.

Langley Research Center
National Aeronautics and Space Administration
Hampton, VA 23665
September 27, 1976

APPENDIX

DEVELOPMENT AND VERIFICATION OF BOUNDARY CORRECTIONS ON STRESS-INTENSITY FACTORS FOR THIN PRESSURIZED CYLINDERS

Through Cracks

Folias (ref. 18) and Erdogan and Kibler (ref. 19) have obtained the elastic stress-intensity factors for a longitudinal (axial) through crack in a pressurized cylinder (fig. 1(a)) for $\lambda_t \leq 4.5$. Figure 16 shows the shell-curvature correction (or boundary-correction factor) on stress intensity as a function of λ_t. The symbols are numerical values obtained from reference 19 for $\nu = 1/3$. The shell-curvature correction factor F was determined by

$$F = F_T + \frac{1}{2}|F_B| \tag{18}$$

where F_T is the contribution due to the membrane solution (or normal forces) and F_B is the contribution due to bending. Reference 21 has shown that including one-half of the bending contribution was necessary to correlate crack-growth rates from pressurized cylinders and flat plates. The bending term contributed only about 10 percent to the total correction factor.

The solid curve in figure 16 is an equation chosen herein (eq. (5)) to fit the numerical values. The solid curve was within ±5 percent of the numerical values. Reference 21 has shown that the effect of Poisson's ratio (ν = 0 to 1/2) on the curvature correction was less than 5 percent from the values given in figure 16. Therefore, equation (5) was assumed to apply for any material.

For $\lambda_t > 4.5$, an experimental technique was used herein to verify the applicability of equation (5) for calculating the shell-curvature correction factors. Figure 17 shows the shell-curvature correction factor plotted against λ_t. The symbols show the experimentally derived correction factors from through-crack fracture data on brass cylinders (ref. 16) using the two-parameter fracture criterion. The correction factors are given by

$$F = f_t = \frac{K_F\left(1 - m\,\frac{S_n}{S_u}\right)}{S_n\sqrt{\pi c}} \tag{19}$$

The fracture parameters K_F and m were determined from an analysis of the fracture data with $\lambda_t \leq 4$. The crack length c and the corresponding failure stresses S_n were obtained from reference 16. The solid curve shows the correction factors calculated from equation (5), and these factors

are in good agreement with the experimental data. Therefore, equation (5) was assumed to apply for any material with $\lambda_t \leqq 10$.

Surface Cracks

Derby (ref. 17) has experimentally determined stress-intensity correction factors for surface cracks in pressurized cylinders made of a brittle epoxy. The critical elastic stress-intensity factor for this material ($K_{Ie} = 1.02$ MN/m$^{3/2}$) was obtained from four-point notch bend fracture tests (ref. 17). This material was brittle ($m = 0$). The experimental correction factors for the surface cracks were obtained from equation (3) as

$$F = \frac{K_{Ie}}{S_n\sqrt{\pi c}} = \frac{1.02}{S_n\sqrt{\pi c}} \tag{20}$$

where S_n and c were obtained from the fracture tests on the epoxy vessels. Table II shows a comparison between the experimentally determined boundary correction factors and those calculated from equation (6). The theoretical correction factors were within ±10 percent of the experimental values.

REFERENCES

1. Brown, William F., Jr.; and Srawley, John E.: Plane Strain Crack Toughness Testing of High Strength Metallic Materials. Spec. Tech. Publ. No. 410, American Soc. Testing & Mater., c.1966.

2. Fracture Toughness Testing and Its Applications. ASTM Spec. Tech. Publ. No. 381, c.1965.

3. Kuhn, Paul: Residual Tensile Strength in the Presence of Through Cracks or Surface Cracks. NASA TN D-5432, 1970.

4. Newman, J. C., Jr.: Fracture Analysis of Surface- and Through-Cracked Sheets and Plates. Eng. Fract. Mech., vol. 5, no. 3, Sept. 1973, pp. 667-689.

5. Newman, J. C., Jr.: Plane-Stress Fracture of Compact and Notch-Bend Specimens. NASA TM X-71926, 1974.

6. Newman, J. C., Jr.: Fracture Analysis of Various Cracked Configurations in Sheet and Plate Materials. NASA TM X-72709, 1975.

7. Newman, J. C., Jr.: Predicting Failure of Specimens With Either Surface Cracks or Corner Cracks at Holes. NASA TN D-8244, 1976.

8. Peters, Roger W.; and Kuhn, Paul: Bursting Strength of Unstiffened Pressure Cylinders With Slits. NACA TN 3993, 1957.

9. Anderson, Robert B.; and Sullivan, Timothy L.: Fracture Mechanics of Through-Cracked Cylindrical Pressure Vessels. NASA TN D-3252, 1966.

10. Sullivan, Timothy L.; and Pierce, William S.: Effect of Radius on Bulging and Fracture of Through-Cracked Cylindrical Pressure Vessels at Cryogenic Temperatures. NASA TN D-4951, 1968.

11. Pierce, William S.: Effects of Surface and Through Cracks on Failure of Pressurized Thin-Walled Cylinders of 2014-T6 Aluminum. NASA TN D-6099, 1970.

12. Sullivan, Timothy L.: Texture Strengthening and Fracture Toughness of Titanium Alloy Sheet at Room and Cryogenic Temperatures. NASA TN D-4444, 1968.

13. Calfo, Frederick D.: Effect of Residual Stress on Fracture Strength of AISI 301 Stainless-Steel and Ti-5Al-2.5Sn ELI Titanium Cracked Thin-Wall Cylinders. NASA TN D-4777, 1968.

14. Kiefner, J. F.; Maxey, W. A.; Eiber, R. J.; and Duffy, A. R.: Failure Stress Levels of Flaws in Pressurized Cylinders. Progress in Flaw Growth and Fracture Toughness Testing, ASTM Spec. Tech. Publ. 536, c.1973, pp. 461-481.

15. Hahn, G. T.; Sarrate, M.; and Rosenfield, A. R.: Criteria for Crack Extension in Cylindrical Pressure Vessels. Int. J. Fract. Mech., vol. 5, no. 3, Sept. 1969, pp. 187-210.

16. Sechler, E. E.; and Williams, M. L.: The Critical Crack Length in Pressurized, Monococque Cylinders. GALCIT 96 (Contract NAw-6525), Grad. Aeronaut. Lab., California Inst. Technol., Sept. 1959.

17. Derby, R. W.: Experimentally Determined Shape Factors for Deep Part-Through Cracks in a Thick-Walled Pressure Vessel. Progress in Flaw Growth and Fracture Toughness Testing, Spec. ASTM Tech. Publ. 536, c.1973, pp. 482-491.

18. Folias, E. S.: An Axial Crack in a Pressurized Cylindrical Shell. Int. J. Fract. Mech., vol. 1, no. 2, June 1965, pp. 104-113.

19. Erdogan, F.; and Kibler, J. J.: Cylindrical and Spherical Shells With Cracks. Int. J. Fract. Mech., vol. 5, no. 3, Sept. 1969, pp. 229-237.

20. Irwin, G. R.: Crack-Extension Force for a Part-Through Crack in a Plate. Trans. ASME, Ser. E: J. Appl. Mech., vol. 29, no. 4, Dec. 1962, pp. 651-654.

21. Erdogan, F.; and Ratwani, M.: Fracture of Cylindrical and Spherical Shells Containing a Crack. Nucl. Eng. & Des., vol. 20, no. 1, 1972, pp. 265-286.

TABLE I.- MATERIALS, THICKNESSES, TEST TEMPERATURES, AND CRACK CONFIGURATIONS

Material	Thickness, mm	Temperature, K	Pressurized cylinders		Flat plates, through crack	Reference
			Surface crack	Through crack		
Aluminum alloy:						
7075-T6	0.4 to 0.6	[a]RT		[b]X		8
2024-T3	0.3 to 0.4	RT		[b]X		8
2014-T6	1.5	RT		[b]X		9
2014-T6	1.5	20		X	X	10
2014-T6	1.5	77		X	X	10
2014-T6	1.5	77	X			11
Titanium alloy:						
Ti-5Al-2.5Sn (ELI)	0.5	20		X	X	10
Ti-5Al-2.5Sn (ELI)	.5	77		X	X	12
Steel:						
AISI 301	0.6	RT		X		13
X-52	9.5	RT		[b]X		14
X-52	9.5	RT	[b]X			14
Hot-rolled[c]	6.4	77		X	X	
Brass	0.025	RT		[b]X		16
Brittle epoxy	15	RT	X			17

[a]Room temperature.
[b]Sharp saw-cut slits instead of fatigue cracks.
[c]0.25C, 0.02Si, 0.85Mn.

TABLE II.- THEORETICALLY AND EXPERIMENTALLY DETERMINED BOUNDARY-CORRECTION FACTORS FOR SURFACE CRACKS IN PRESSURIZED CYLINDERS MADE OF A BRITTLE EPOXY

[R = 68.3 mm and t = 15 mm (from ref. 17)]

a, mm	c, mm	Experimental F	Theoretical F	$\frac{\text{Theoretical F}}{\text{Experimental F}}$
13.2	14.6	0.959	0.932	0.97
12.2	14.2	.878	.863	.98
11.1	14.5	.846	.855	1.01
10.9	14.5	.846	.823	.97
10.5	15.9	.808	.841	1.04
11.5	14.4	.831	.839	1.01
10.7	14.5	.785	.819	1.04
6.9	9.5	.682	.696	1.02
6.9	8.3	.708	.689	.97
7.3	8.3	.672	.689	1.03
5.4	8.5	.621	.677	1.09

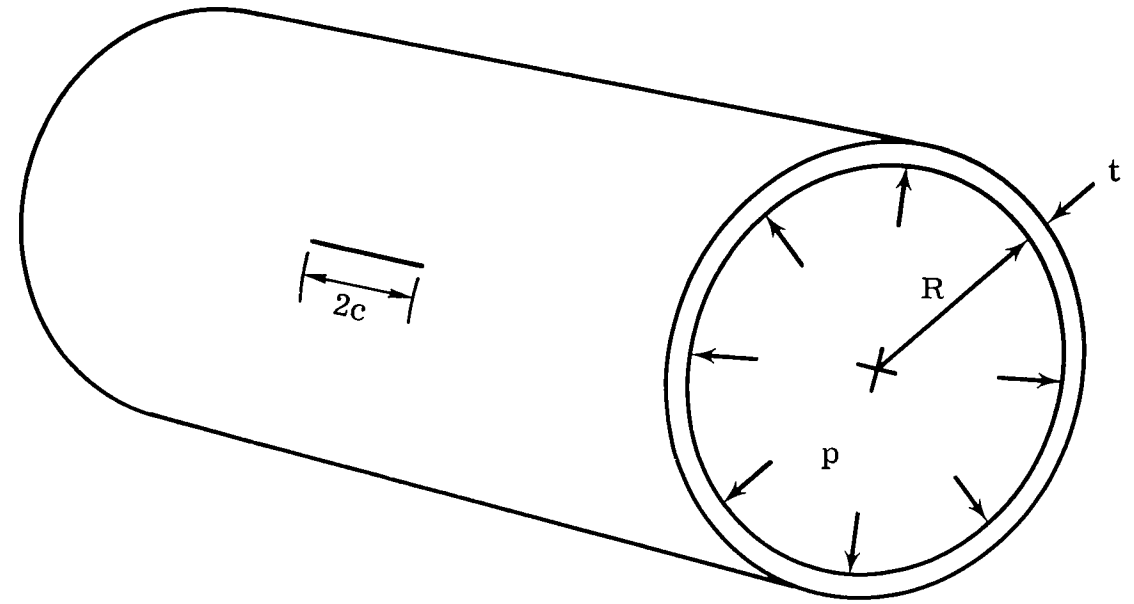

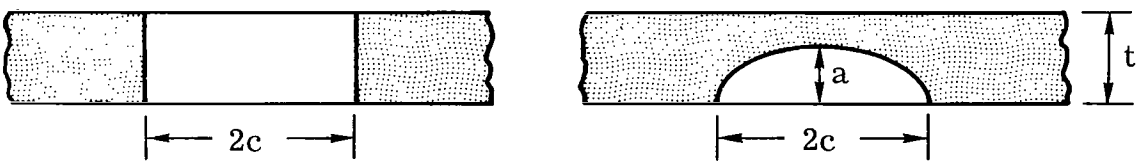

(a) Through crack. (b) Surface crack.

Figure 1.- Surface crack or a through crack in a pressurized cylinder.

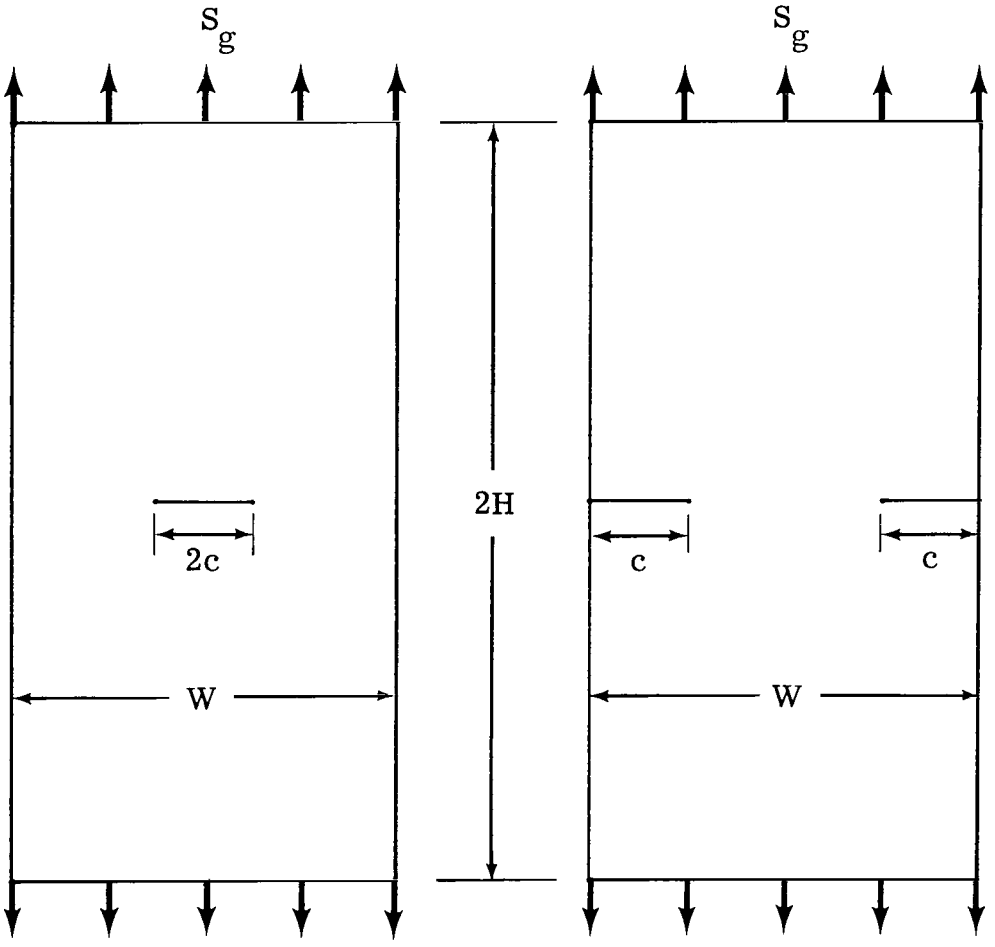

(a) Center-crack tension. (b) Double-edge-crack tension.

Figure 2.- Through-crack configurations in flat plates.

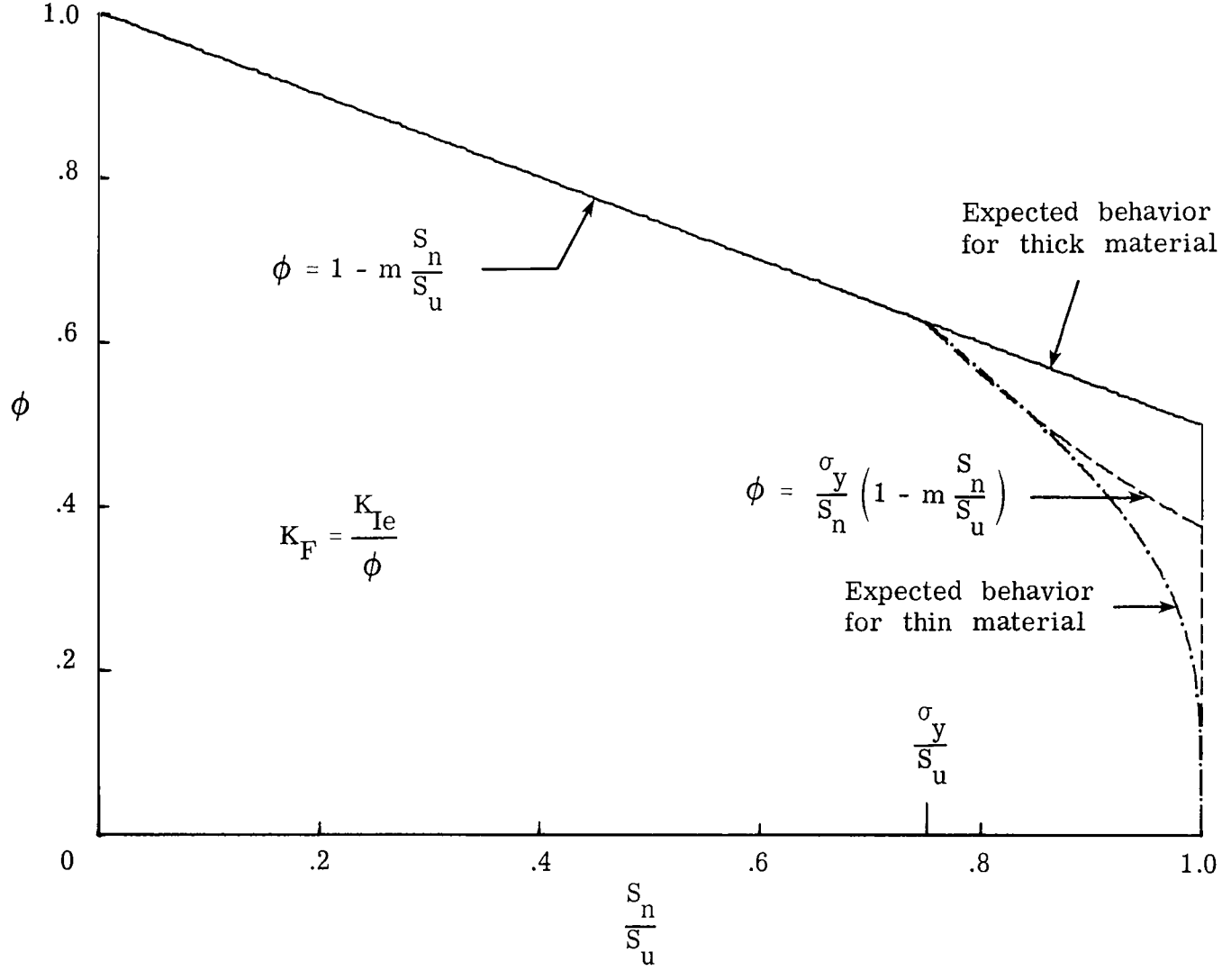

Figure 3.- Typical relationship between ϕ and S_n/S_u.

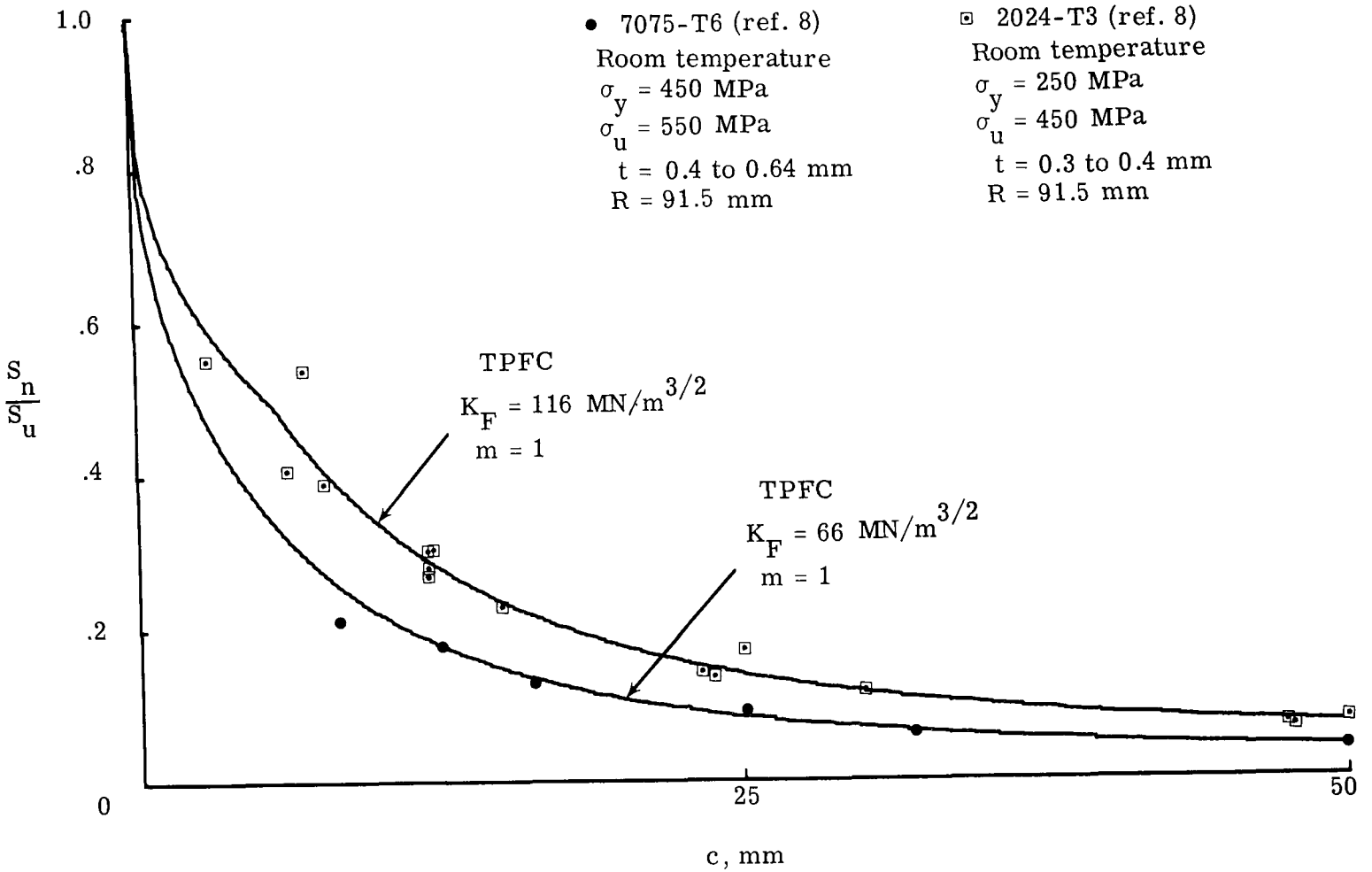

Figure 4.- Nominal failure stresses for through cracks in pressurized cylinders made of 7075-T6 and 2024-T3 aluminum alloy.

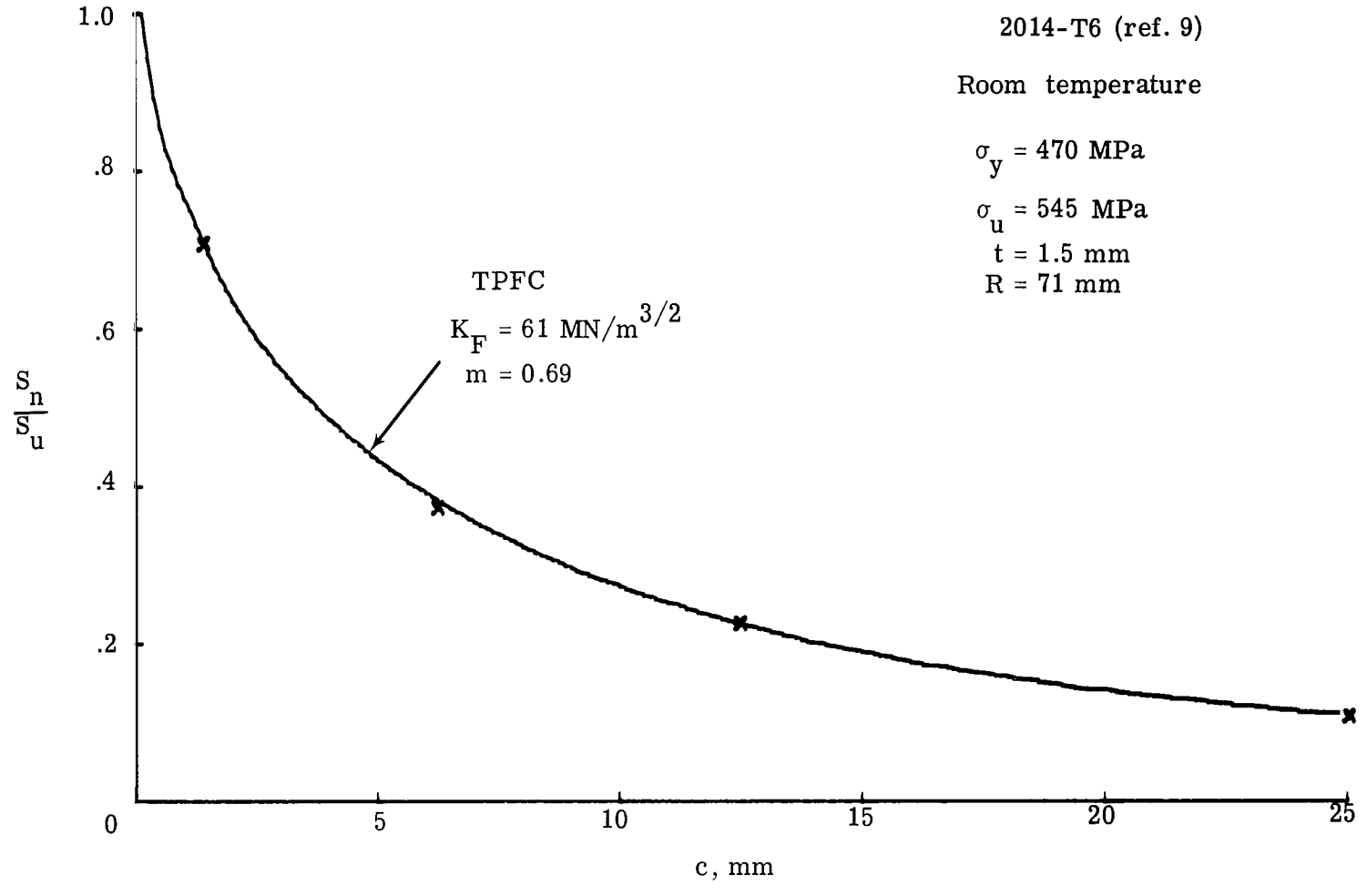

Figure 5.- Nominal failure stresses for through cracks in pressurized cylinders made of 2014-T6 aluminum alloy.

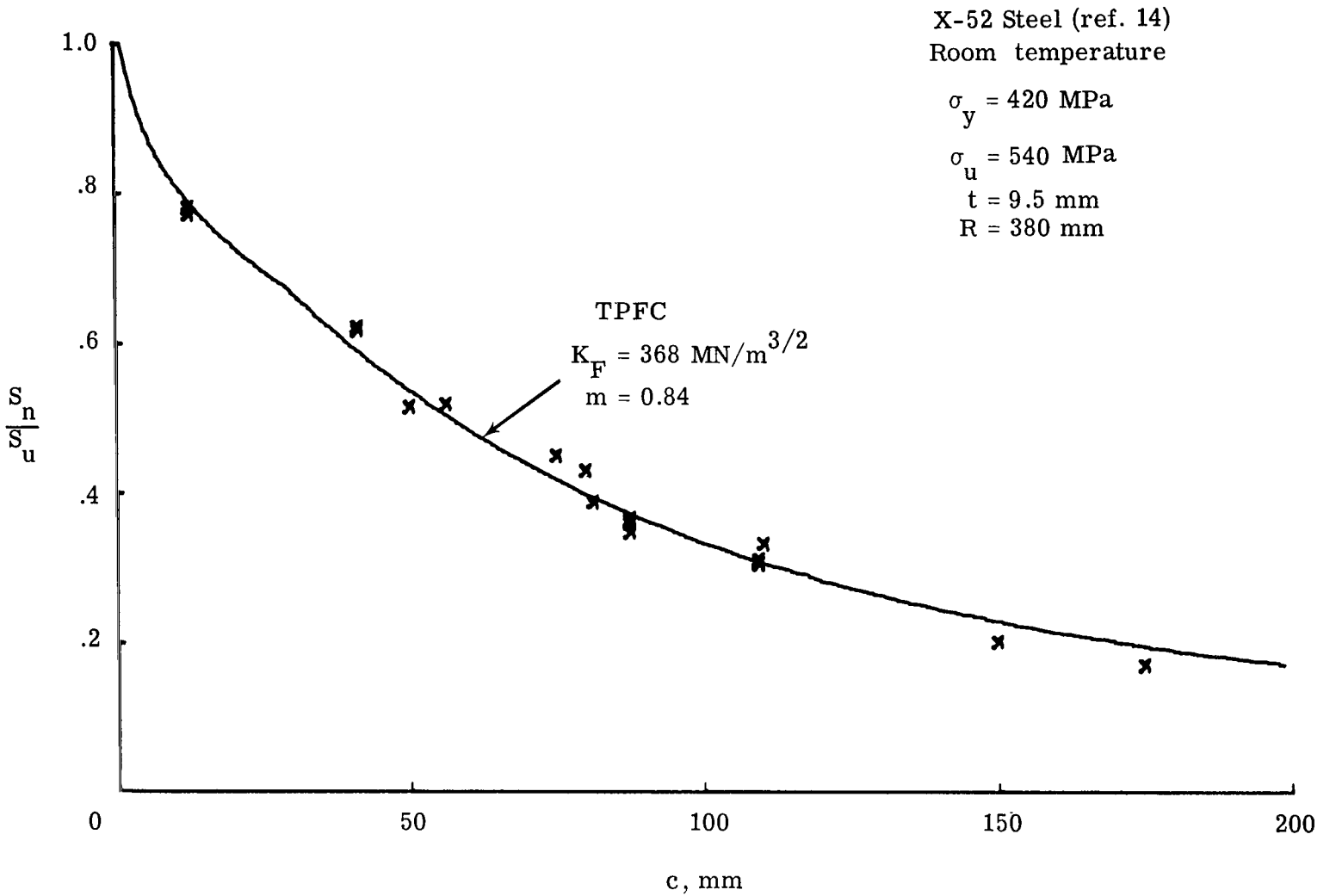

Figure 6.- Nominal failure stresses for through cracks in pressurized cylinders made of X-52 steel.

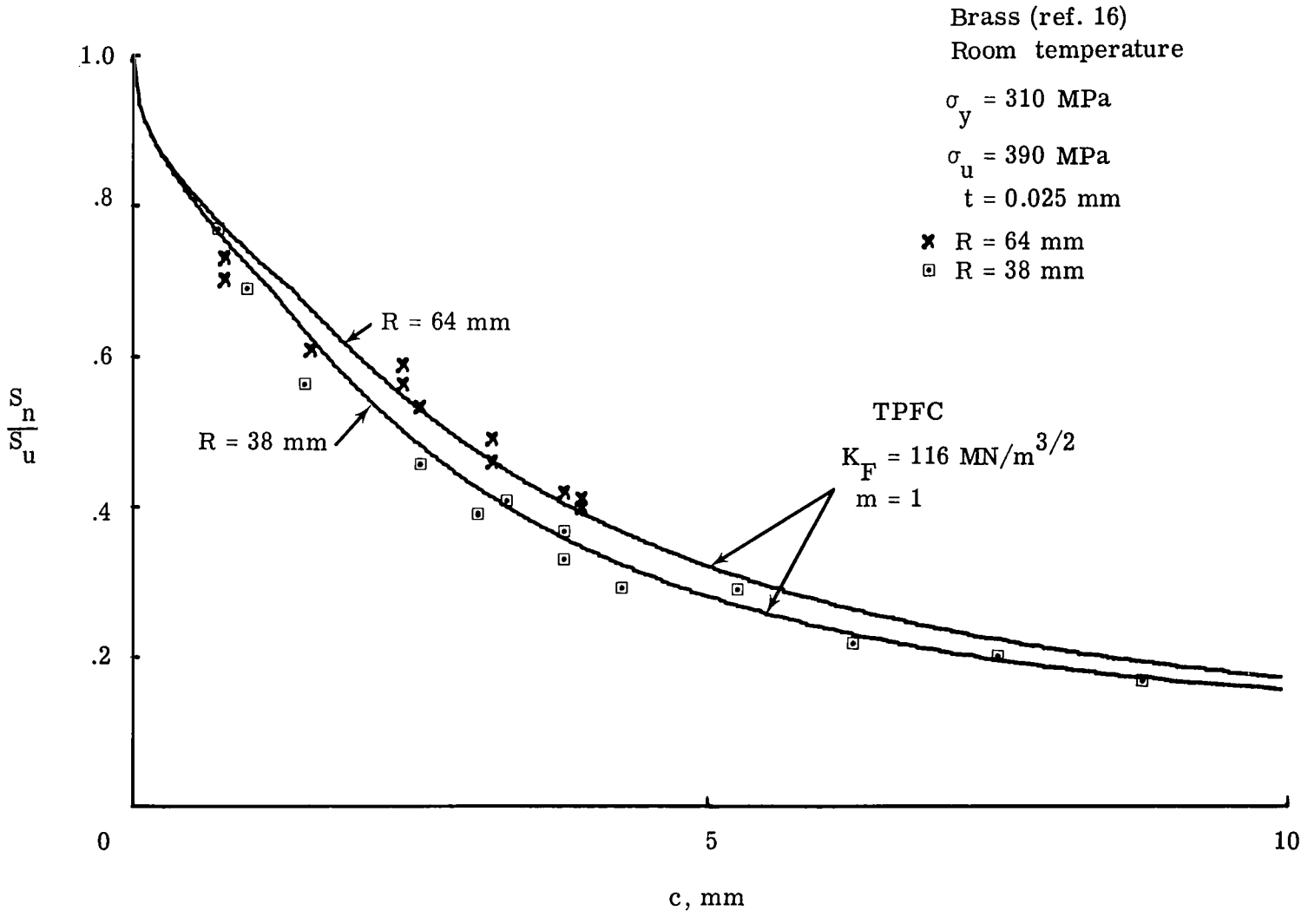

Figure 7.- Nominal failure stresses for through cracks in pressurized cylinders made of brass.

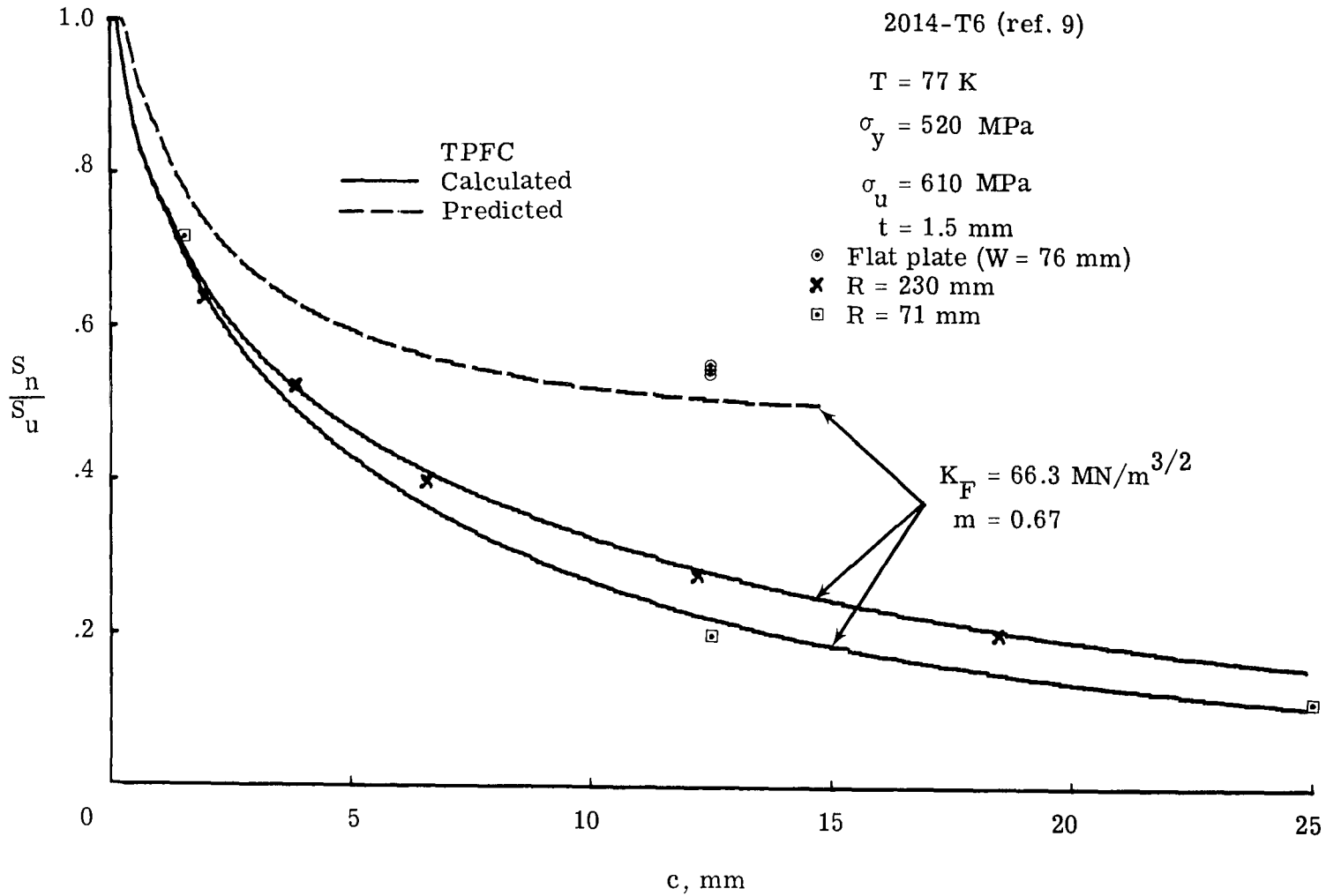

Figure 8.- Nominal failure stresses for through cracks in flat plates and pressurized cylinders made of 2014-T6 aluminum alloy.

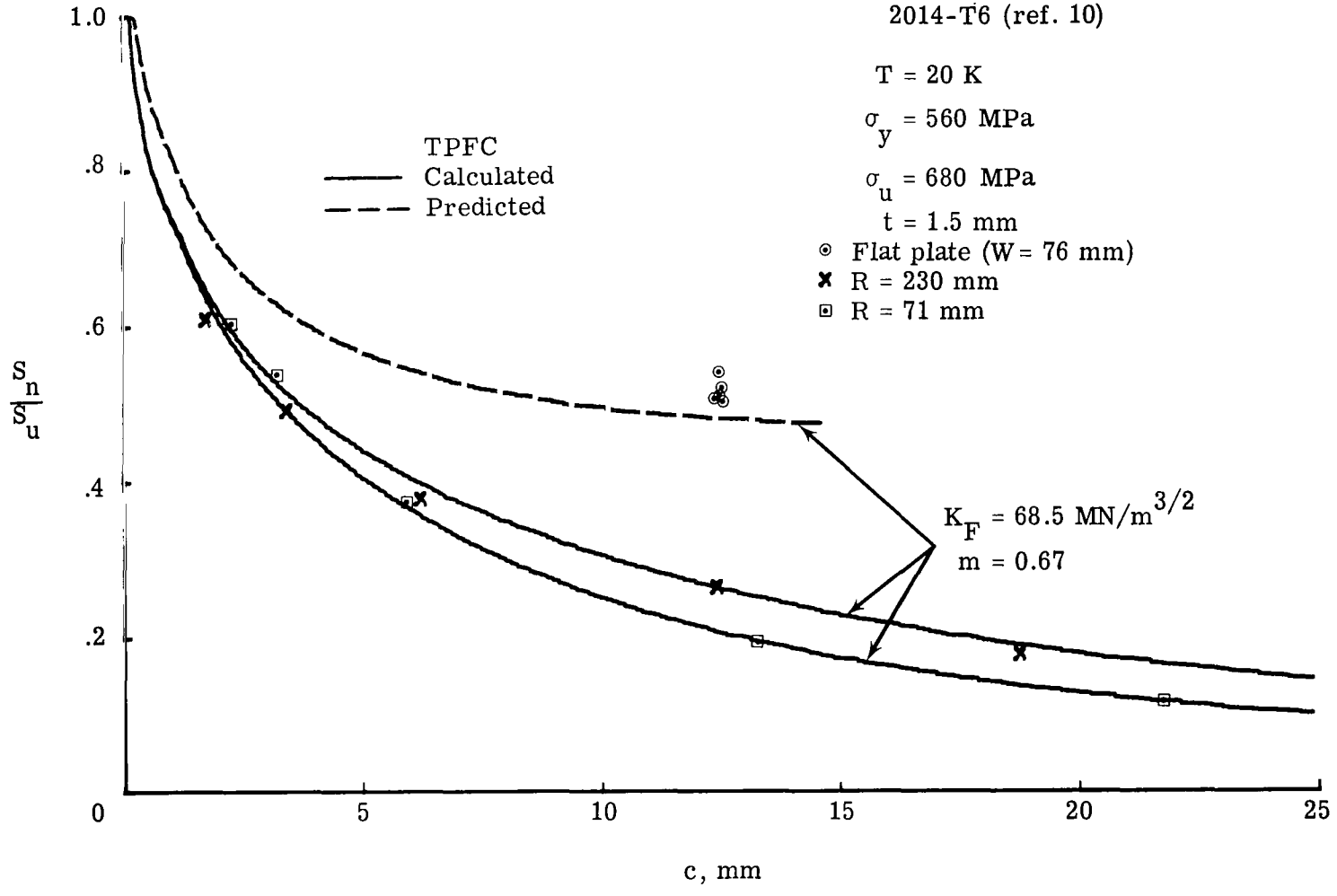

Figure 9.- Nominal failure stresses for through cracks in flat plates and pressurized cylinders made of 2014-T6 aluminum alloy.

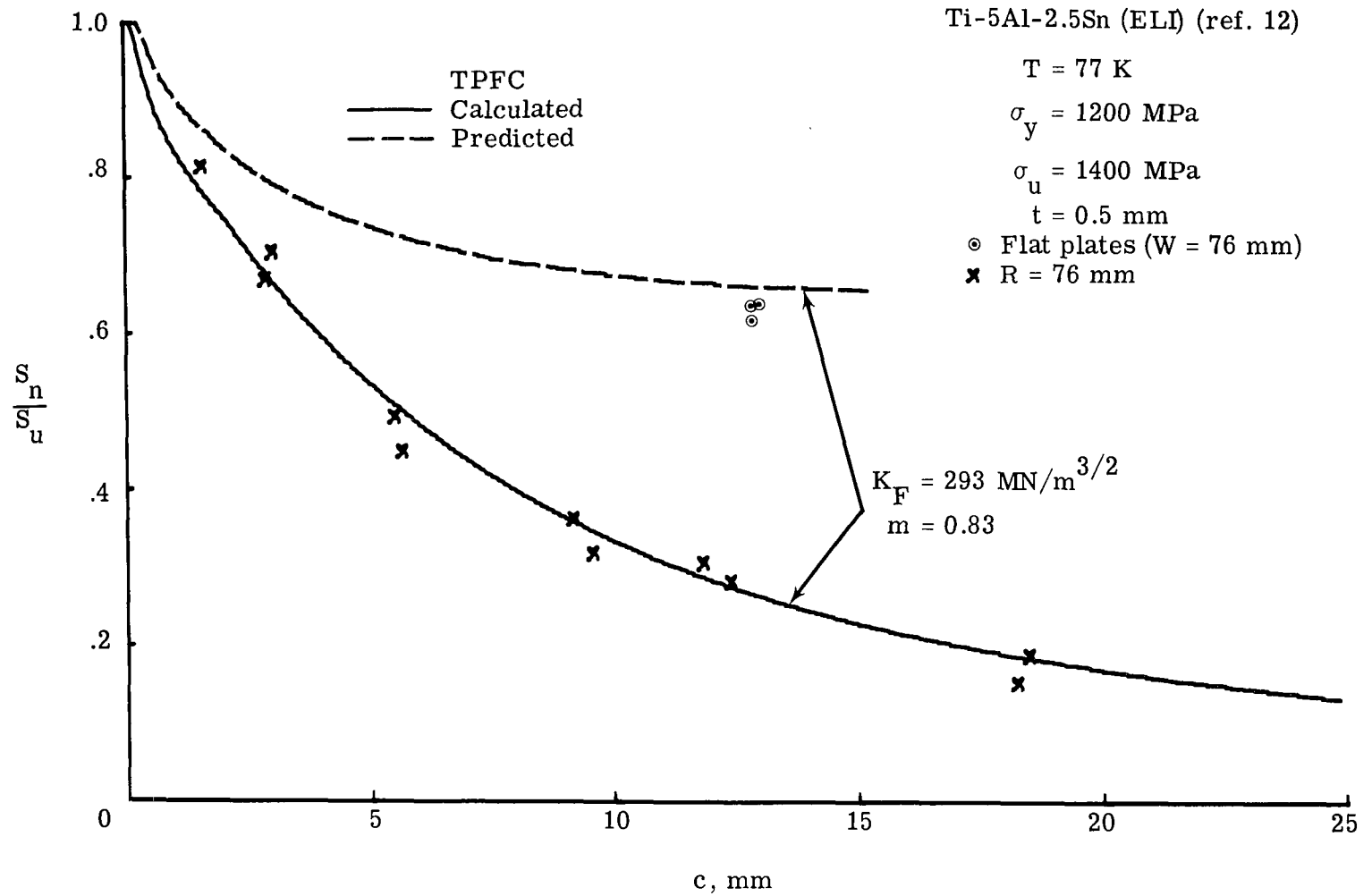

Figure 10.- Nominal failure stresses for through cracks in flat plates and pressurized cylinders made of Ti-5Al-2.5Sn (ELI) titanium alloy.

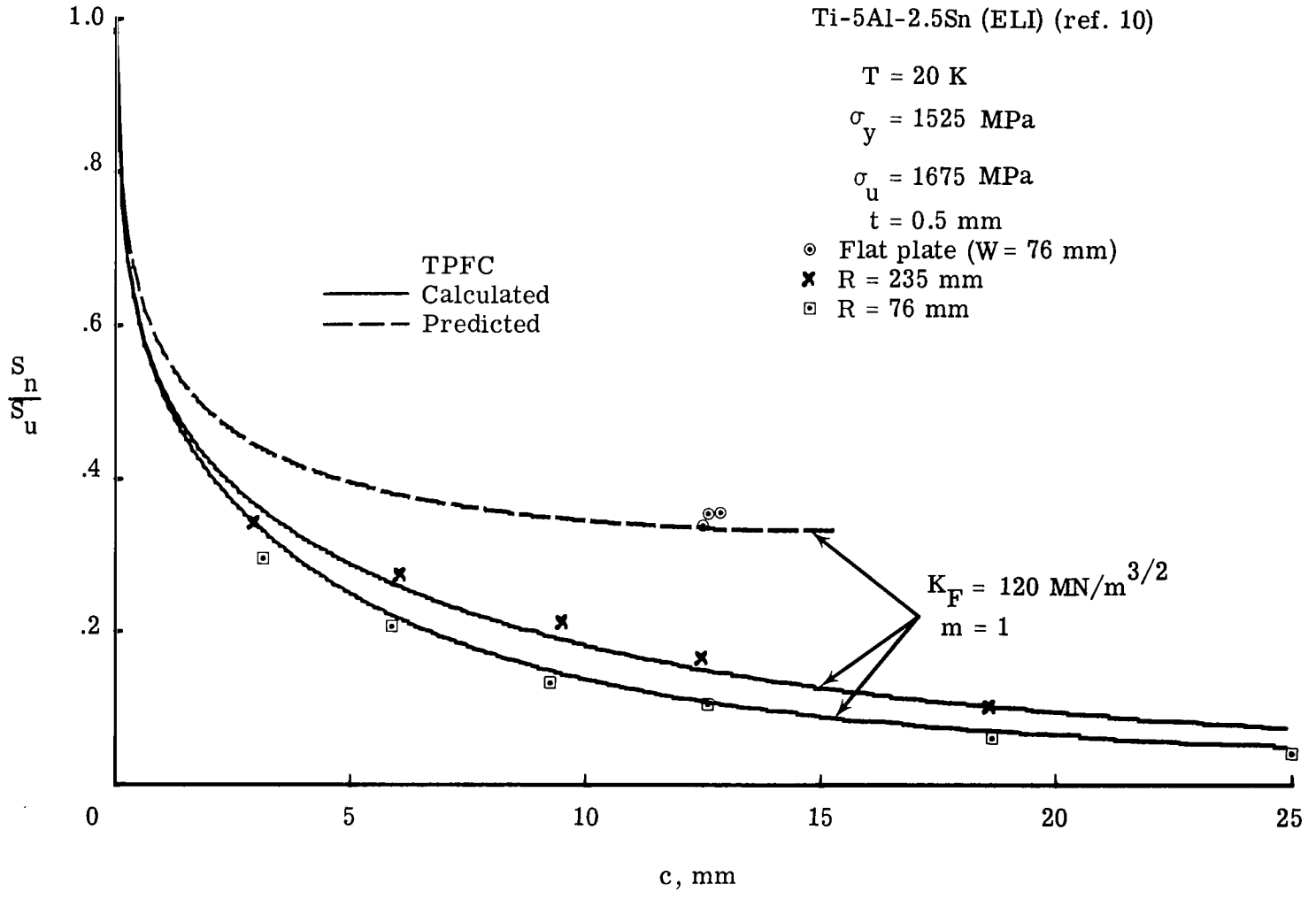

Figure 11.- Nominal failure stresses for through cracks in flat plates and pressurized cylinders made of Ti-5Al-2.5Sn (ELI) titanium alloy.

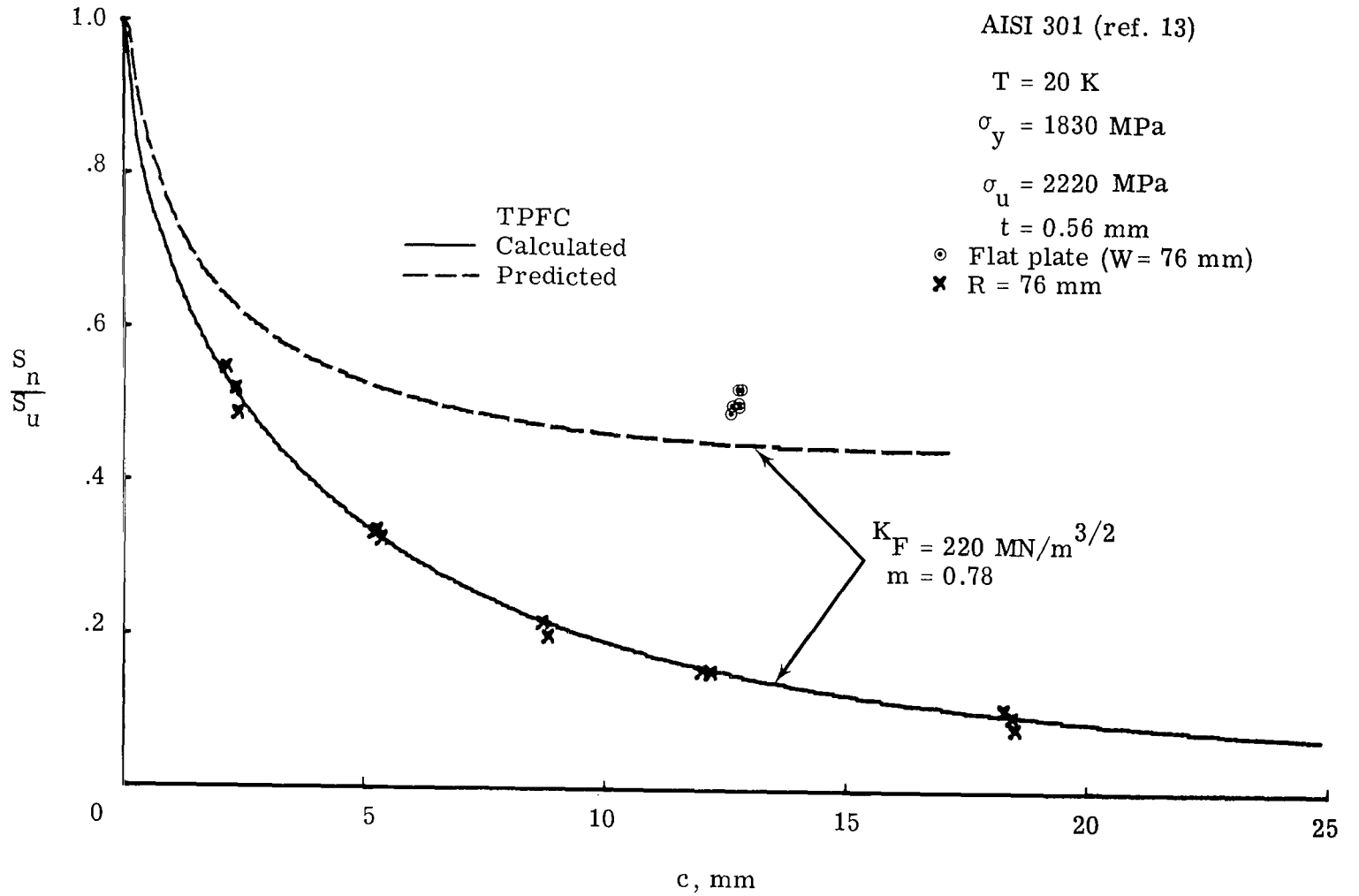

Figure 12.- Nominal failure stresses for through cracks in flat plates and pressurized cylinders made of AISI 301 stainless steel.

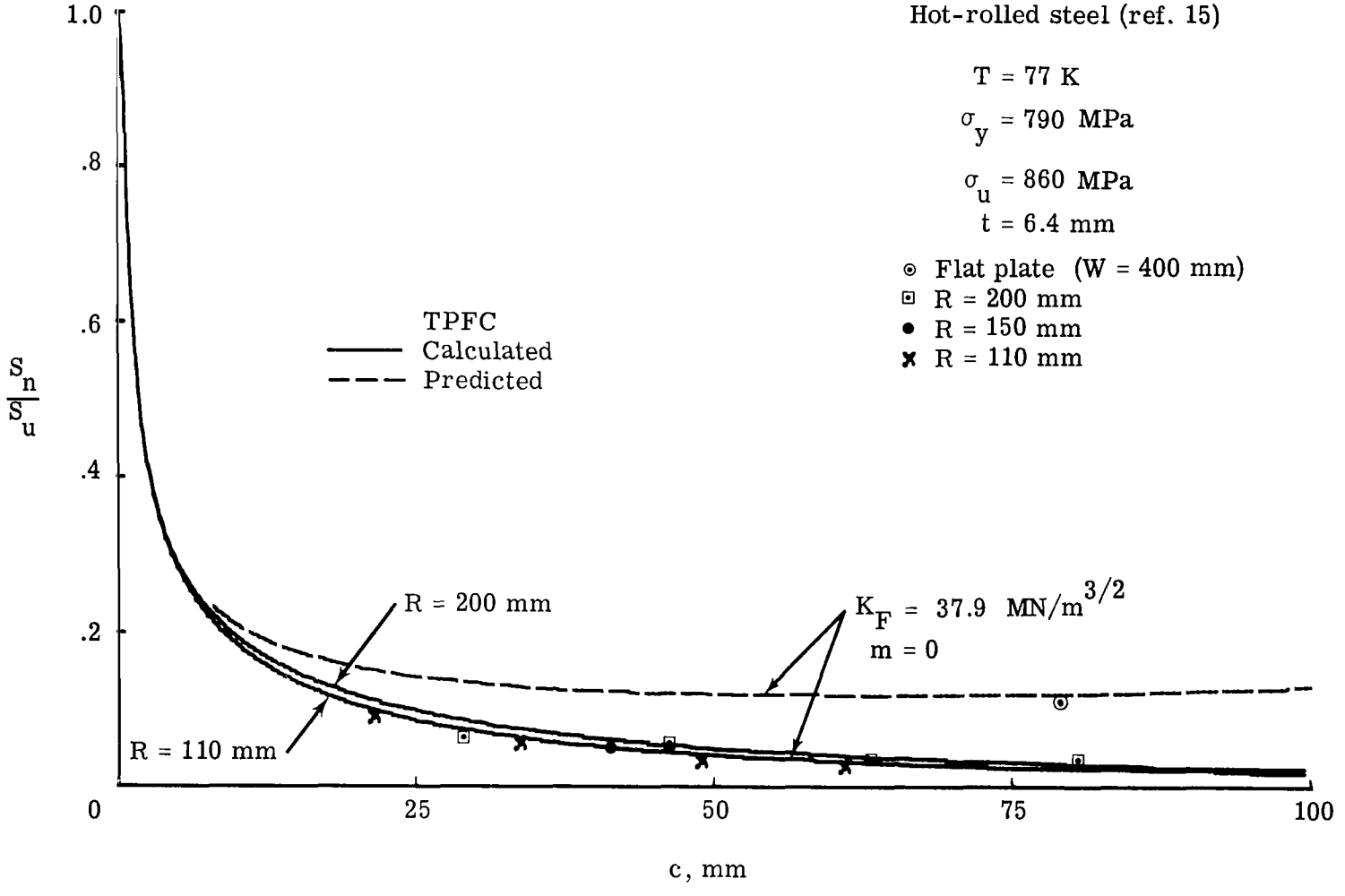

Figure 13.- Nominal failure stresses for through cracks in flat plates and pressurized cylinders made of hot-rolled steel.

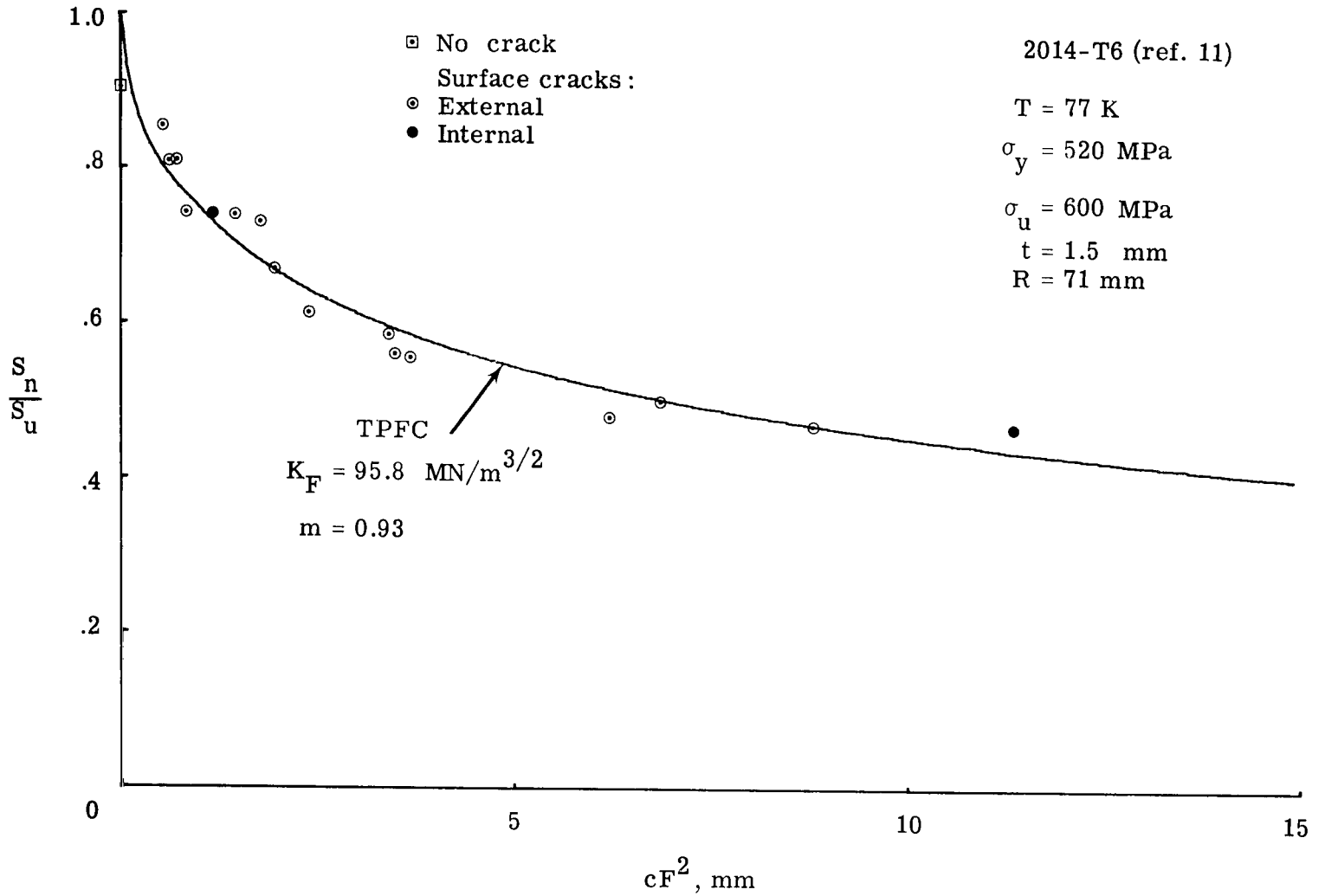

Figure 14.- Nominal failure stresses for surface cracks in pressurized cylinders made of 2014-T6 aluminum alloy.

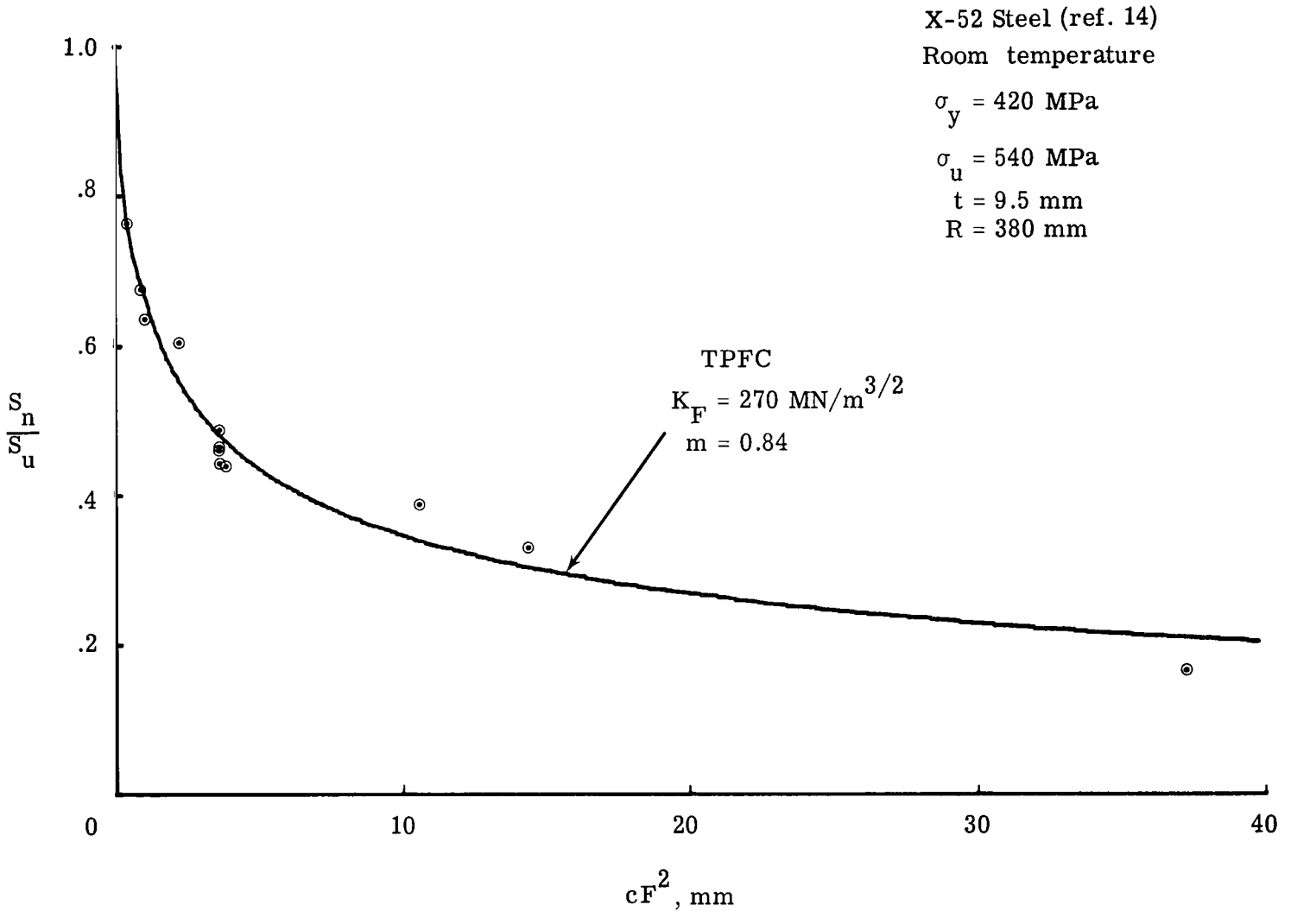

Figure 15.- Nominal failure stresses for surface cracks in pressurized cylinders made of X-52 steel.

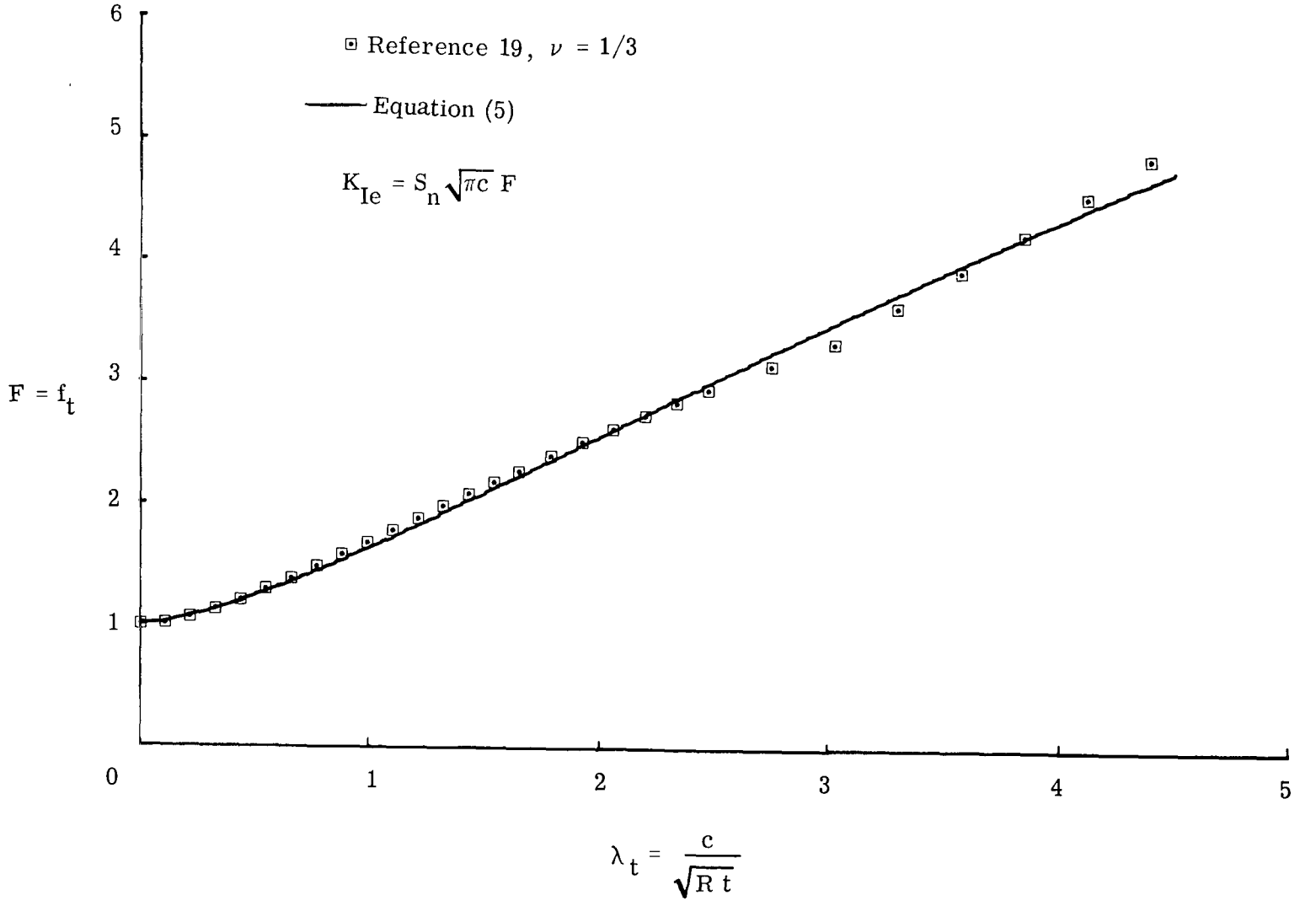

Figure 16.- Shell-curvature correction factors for an axial through crack in a pressurized cylinder.

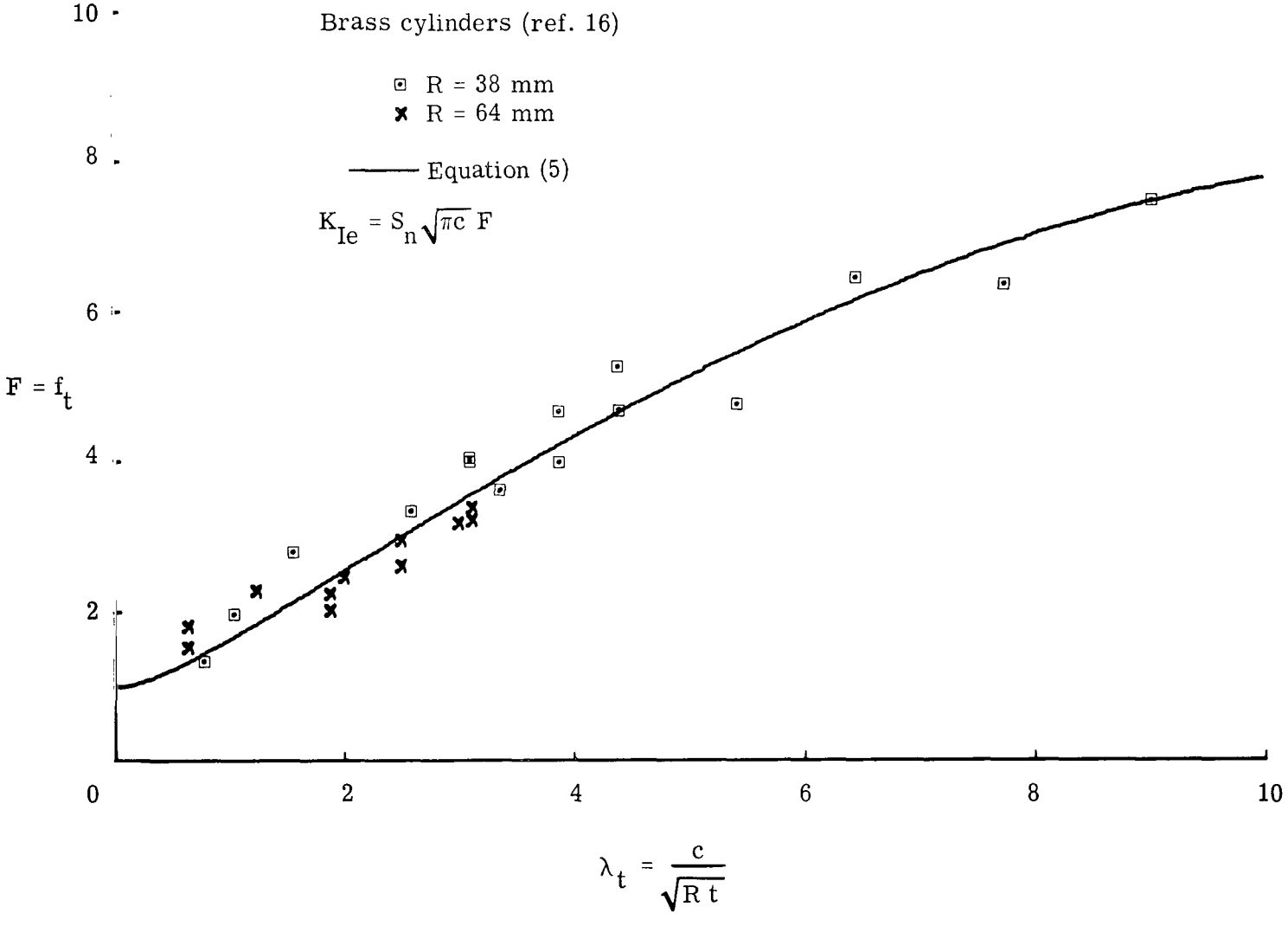

Figure 17.- Experimental and theoretical shell-curvature correction factors for an axial through crack in a pressurized cylinder.

827 001 C1 U D 761008 S00903DS
DEPT OF THE AIR FORCE
AF WEAPONS LABORATORY
ATTN: TECHNICAL LIBRARY (SUL)
KIRTLAND AFB NM 87117

"The aeronautical and space activities of the United States shall be conducted so as to contribute . . . to the expansion of human knowledge of phenomena in the atmosphere and space. The Administration shall provide for the widest practicable and appropriate dissemination of information concerning its activities and the results thereof."

—NATIONAL AERONAUTICS AND SPACE ACT OF 1958

NASA SCIENTIFIC AND TECHNICAL PUBLICATIONS

TECHNICAL REPORTS: Scientific and technical information considered important, complete, and a lasting contribution to existing knowledge.

TECHNICAL NOTES: Information less broad in scope but nevertheless of importance as a contribution to existing knowledge.

TECHNICAL MEMORANDUMS: Information receiving limited distribution because of preliminary data, security classification, or other reasons. Also includes conference proceedings with either limited or unlimited distribution.

CONTRACTOR REPORTS: Scientific and technical information generated under a NASA contract or grant and considered an important contribution to existing knowledge.

TECHNICAL TRANSLATIONS: Information published in a foreign language considered to merit NASA distribution in English.

SPECIAL PUBLICATIONS: Information derived from or of value to NASA activities. Publications include final reports of major projects, monographs, data compilations, handbooks, sourcebooks, and special bibliographies.

TECHNOLOGY UTILIZATION PUBLICATIONS: Information on technology used by NASA that may be of particular interest in commercial and other non-aerospace applications. Publications include Tech Briefs, Technology Utilization Reports and Technology Surveys.

Details on the availability of these publications may be obtained from:

SCIENTIFIC AND TECHNICAL INFORMATION OFFICE

NATIONAL AERONAUTICS AND SPACE ADMINISTRATION

Washington, D.C. 20546